NRC
Research Press

ARTICLE

Quantifying ^{87}Sr/^{86}Sr temporal stability and spatial heterogeneity for use in tracking fish movement

Lindsy R. Ciepiela and Annika W. Walters

Abstract: The specificity and accuracy of inferred fish origin and movement relies on describing spatial heterogeneity and temporal stability of environmental signatures. But the cost and logistics of sample collection often precludes the complete quantification of environmental signature temporal stability and spatial heterogeneity. We used repeated sampling and a novel approach (Bayesian ridge regression, BRR) to quantify the temporal stability and spatial heterogeneity of ^{87}Sr/^{86}Sr, respectively. We explained 86% of observed variation in ^{87}Sr/^{86}Sr using a BRR model and estimated ^{87}Sr/^{86}Sr throughout the Upper North Platte River Basin with high accuracy (±0.00106). Year to year variation in ^{87}Sr/^{86}Sr signatures ranged from 0.00007 to 0.00073 (SD), while seasonal variation ranged from 0.00091 to 0.00134 (SD). We then assessed the specificity and discussed the accuracy of inferring movement using three scenarios of described spatial heterogeneity. Our results indicate reliable inference of fish movement requires comprehensive quantification of spatial heterogeneity and temporal variation in environmental signatures.

Résumé : La spécificité et l'exactitude de l'origine et des déplacements inférés de poissons reposent sur la description de l'hétérogénéité spatiale et de la stabilité temporelle de signatures environnementales. En raison du coût et de la logistique du prélèvement d'échantillons, il est souvent impossible d'arriver à une quantification exhaustive de ces facteurs. Nous utilisons l'échantillonnage répété et une nouvelle approche (la régression ridge bayésienne, RRB) pour quantifier, respectivement, la stabilité temporelle et l'hétérogénéité spatiale du rapport ^{87}Sr/^{86}Sr. Nous expliquons 86 % de la variation de ^{87}Sr/^{86}Sr observée en utilisant un modèle de RRB et estimons ^{87}Sr/^{86}Sr à la grandeur du bassin supérieur de la rivière North Platte avec une exactitude élevée (±0,00106). La variation interannuelle des signatures de ^{87}Sr/^{86}Sr va de 0,00007 à 0,00073 (ÉT) et la variation saisonnière, de 0,00091 à 0,00134 (ÉT). Nous évaluons ensuite la spécificité et abordons l'exactitude des déplacements inférés en utilisant trois scénarios d'hétérogénéité spatiale décrite. Les résultats indiquent que l'inférence fiable des déplacements de poissons nécessite la quantification exhaustive de l'hétérogénéité spatiale et de la variation temporelle de signatures environnementales. [Traduit par la Rédaction]

Introduction

Fish move 10s–1000s of kilometres to satisfy physiological requirements such as spawning, feeding, and growth (Gross et al. 1988; see Binder et al. 2011). Knowing fish origin, their migration routes, and the habitats associated with their growth and reproduction is fundamental to the successful conservation of desired species and the control of undesired species (Munro et al. 2005; Olden et al. 2006; see Cooke et al. 2012). As such, considerable effort has been put forth to develop techniques that allow for the tracking of fish movement (Lucas and Baras 2000). Studies that have used artificial tagging techniques, such as passive integrated transponder tags, radio transmitters, and visible implant elastomer marks, have contributed to our understanding of fish spatial ecology (Achord et al. 2007; Hutchison et al. 2008). Yet our understanding of fish movement has been limited due to logistical difficulties in tagging juvenile fish, recovering long-distance migrants, and monitoring movement through time (Young et al. 1997; Kanno et al. 2014).

Over the last two decades, technological advances in methods for analyzing otolith microchemistry have allowed researchers to overcome many of the limitations of conventional tagging techniques for assessing fish movement (see Elsdon et al. 2008). By analyzing environmental signatures across a fish's otolith and matching signatures to surface water environmental signatures, researchers can reconstruct the environmental history of all life stages of fishes over large spatial and temporal scales. Studies that use otolith microchemistry have identified essential habitat for juvenile fish (e.g., Dorval et al. 2005; Brown 2006), characterized within-population life history diversity (e.g., Zlokovitz et al. 2003; Hodge et al. 2016), and identified the source of invasive species (e.g., Munro et al. 2005; Whitledge et al. 2007).

Otolith microchemistry has increased our understanding of fish movement dynamics and habitat needs, but is not without its own set of assumptions and limitations (Elsdon et al. 2008). Studies that use otolith microchemistry to trace movement are typically based on at least two key assumptions — (*i*) detectable differences in surface water environmental signatures occur on a scale relevant to fish movement, and (*ii*) surface water environmental signatures are temporally consistent. While these assumptions are well recognized, budget and logistical constraints often limit full quantification of spatial and temporal variation in environmental signatures, especially given competing demands of a study (e.g., fish and water collections). Failure to capture environmental variation can influence the accuracy (i.e., the true stream the fish was occupying is identified) and spatial resolution of inferred movement histories. Therefore, there is a need to quantify the temporal

L.R. Ciepiela. Wyoming Cooperative Fish and Wildlife Research Unit, Department of Zoology and Physiology, University of Wyoming, Laramie, WY 82071, USA.
A.W. Walters. US Geological Survey, Wyoming Cooperative Fish and Wildlife Research Unit, Department of Zoology and Physiology, University of Wyoming, Laramie, WY 82071, USA.
Corresponding author: Lindsy R. Ciepiela (email: lrciepie@gmail.com).

stability of environmental signatures and develop cost-effective methods to quantify the spatial variation of environmental signatures.

In freshwater environments, water strontium isotope ratios ($^{87}Sr/^{86}Sr$) are a useful environmental signature for reconstructing environmental histories of fishes (Gibson-Reinemer et al. 2009). $^{87}Sr/^{86}Sr$ measured in otoliths are tightly correlated with $^{87}Sr/^{86}Sr$ measured in ambient fresh waters (Barnett-Johnson et al. 2008; Muhlfeld et al. 2012). $^{87}Sr/^{86}Sr$ in fresh waters, and thus otoliths, are directly influenced by underlying watershed geology, with variation in rock type, age, and weathering rates leading to spatial heterogeneity of $^{87}Sr/^{86}Sr$ (Bataille and Bowen 2012; Bataille et al. 2014). Because $^{87}Sr/^{86}Sr$ signatures are tightly correlated with bedrock geology, modeling techniques that estimate $^{87}Sr/^{86}Sr$ from bedrock geology and landscape variables are a promising, cost-effective technique to quantify $^{87}Sr/^{86}Sr$ spatial heterogeneity across a watershed (Hegg et al. 2013). For example, Brennan et al. (2016) successfully used dendritic network models to estimate strontium values within the Nushagak Basin, Alaska, with high accuracy and spatial resolution.

The objectives of this research were to describe the temporal stability of $^{87}Sr/^{86}Sr$, develop a modeling technique to estimate $^{87}Sr/^{86}Sr$, and assess the specificity (i.e., the number of tributaries a fish is assigned too) and accuracy (i.e., whether a fish is assigned to its true stream of origin) of inferring fish movement at different levels of quantified $^{87}Sr/^{86}Sr$ spatial variation. We quantified $^{87}Sr/^{86}Sr$ temporal stability through repeated sampling of water $^{87}Sr/^{86}Sr$. We used a machine learning algorithm, Bayesian ridge regression (BRR), to estimate water $^{87}Sr/^{86}Sr$ signatures based on bedrock lithology and landscape processes. We then compared our results with those obtained using the spatial stream network (SSN) modeling technique presented in Brennan et al. (2016). Finally, we used the above data to examine implications of inferring fish movement at different levels of quantified $^{87}Sr/^{86}Sr$ spatial variation.

Materials and methods

Study site

We developed $^{87}Sr/^{86}Sr$ models using surface water samples and associated bedrock geology and landscape covariates from 17 perennial tributaries and the main stem of the North Platte River in the upper 3600 km² of the Upper North Platte River (UNPR) Basin (refer to online Supplementary material, Fig. S1[1]). The North Platte River originates at the confluence of Little Grizzly and Grizzly creeks in Colorado, USA, and flows northwest into Wyoming through the Saratoga Valley where its tributaries drain the Medicine Bow Mountains to the east and the Sierra Madre Mountains to the west. Snowmelt is the main water source during peak springs flows, while groundwater inputs maintain base flows throughout the fall and winter.

The Sierra Madre and Medicine Bow mountains are geologically similar. Both ranges contain a major shear zone, the Cheyenne belt, which separates the oldest Archean rocks to the north from the younger igneous and metamorphic rocks to the south (Taucher et al. 2013). Notably, the Medicine Bow Mountains, unlike the Sierra Madre Mountains, contain a thick band of metasedimentary rocks that form the Snowy Range (Taucher et al. 2013).

Surface water samples

We collected water samples at 59 locations between June and October 2015 (Fig. 1, Fig. S1[1]). Each of the 17 tributaries had one to five collection locations, and the North Platte River had nine collection locations. We limited our sampling locations to watersheds greater than 6 km² and stratified collection locations

longitudinally along tributaries to encompass variation in underlying geology and stream network dynamics.

We collected water samples in 250 mL Nalgene high-density polyethylene bottles and stored samples in a ziplock bag. Within 48 h of collection, we filtered samples through a 0.45 μm sterile syringe filter into a 125 mL Nalgene high-density polyethylene bottle. Samples were transported to the University of Wyoming and refrigerated until analysis. To evaluate error in field collection and filtration methods, we collected six of the samples as field triplicates. At each triplicate sampling location, we took a blank sample using ultrapure water. We precleaned all sample bottles and filtration equipment by washing equipment in a 1.2 mol·L⁻¹ HCl acid bath for at least 12 h followed by three ultrapure water rinses.

We assessed year to year variation of strontium isotope ratios by comparing water samples collected during August base flows in 2009, 2014, and 2015 at one site each on French Creek, Big Creek, Douglas Creek, and the Encampment River and three sites on the North Platte River. We assessed seasonal variation of strontium isotope ratios by comparing water samples collected at one site each on French and Big creeks in June, August, and October 2015 and May 2016. Our May sampling event occurred during snowmelt-dominated spring run-off, and our October sampling event occurred during groundwater-dominated base flows, with the June and August sampling events occurring during the transition between run-off and base flow. We quantified seasonal variation in French and Big creeks because they represented the range of seasonal variation we expected throughout the basin. French Creek drains the Medicine Bow Mountains, and Big Creek drains the Sierra Madre Mountains.

$^{87}Sr/^{86}Sr$ analysis

The 2009 water samples were collected by Wyoming Game and Fish Department and analyzed for $^{87}Sr/^{86}Sr$ and [Sr] at the University of California, Davis, Interdisciplinary Center of Plasma Mass Spectrometry. Two of 14 water samples were ran as duplicates. Duplicate sample analysis revealed a mean ±2 standard deviations (SDs) of 0.0001. The NIST SRM987 standard ($^{87}Sr/^{86}Sr$ = 0.71034 ± 0.00026 95% confidence interval (CI); www.nist.gov) was used to monitor machine drift. During analysis, mean within-run internal error was ±0.000026 (2 standard errors (SEs)).

We sent water samples from 2014 to 2016 to the University of Utah, Department of Geology and Geophysics, Strontium Isotope Laboratory for $^{87}Sr/^{86}Sr$ and [Sr] analysis where they were analyzed using methods outlined in Brennan et al. (2015). Briefly, water samples were analyzed for $^{87}Sr/^{86}Sr$ ratios using multicollector inductively coupled plasma mass spectrometry (Thermo Scientific, High Resolution NEPTUNE, Bremen, Germany) with online purification system (using Sr-spec resin, Eichrom Technologies Inc.) for $^{87}Sr/^{86}Sr$ analysis of aqueous solutions. Long-term replicability of the NIST SRM987 ($^{87}Sr/^{86}Sr$ = 0.71034 ± 0.00026 95% CI; www.nist.gov) is $^{87}Sr/^{86}Sr$ = 0.71030 ± 0.00004 (2 SD) (Brennan et al. 2015). During water sample analysis, the weighted daily mean (±2 SD) of the NIST SRM987 ratio was 0.71029 ± 0.000033 (n = 5). Field triplicate analysis revealed a mean ±2 SD of 0.000055.

For comparison of water samples between labs, we normalized all samples to the NIST SRM987 standard using the following equation:

$$^{87}Sr/^{86}Sr \text{ normalized} = \left(\frac{S_p}{S_m}\right) \times {}^{87}Sr/^{86}Sr$$

where S_p is the published standard value, and S_m is the average measured standard value.

Fig. 1. Surface water ^{87}Sr/^{86}Sr were estimated across the Upper North Platte River Basin using a Bayesian ridge regression model. Solid circles indicate sampling locations. This map was created using ArcGIS software by Esri. [Colour online.]
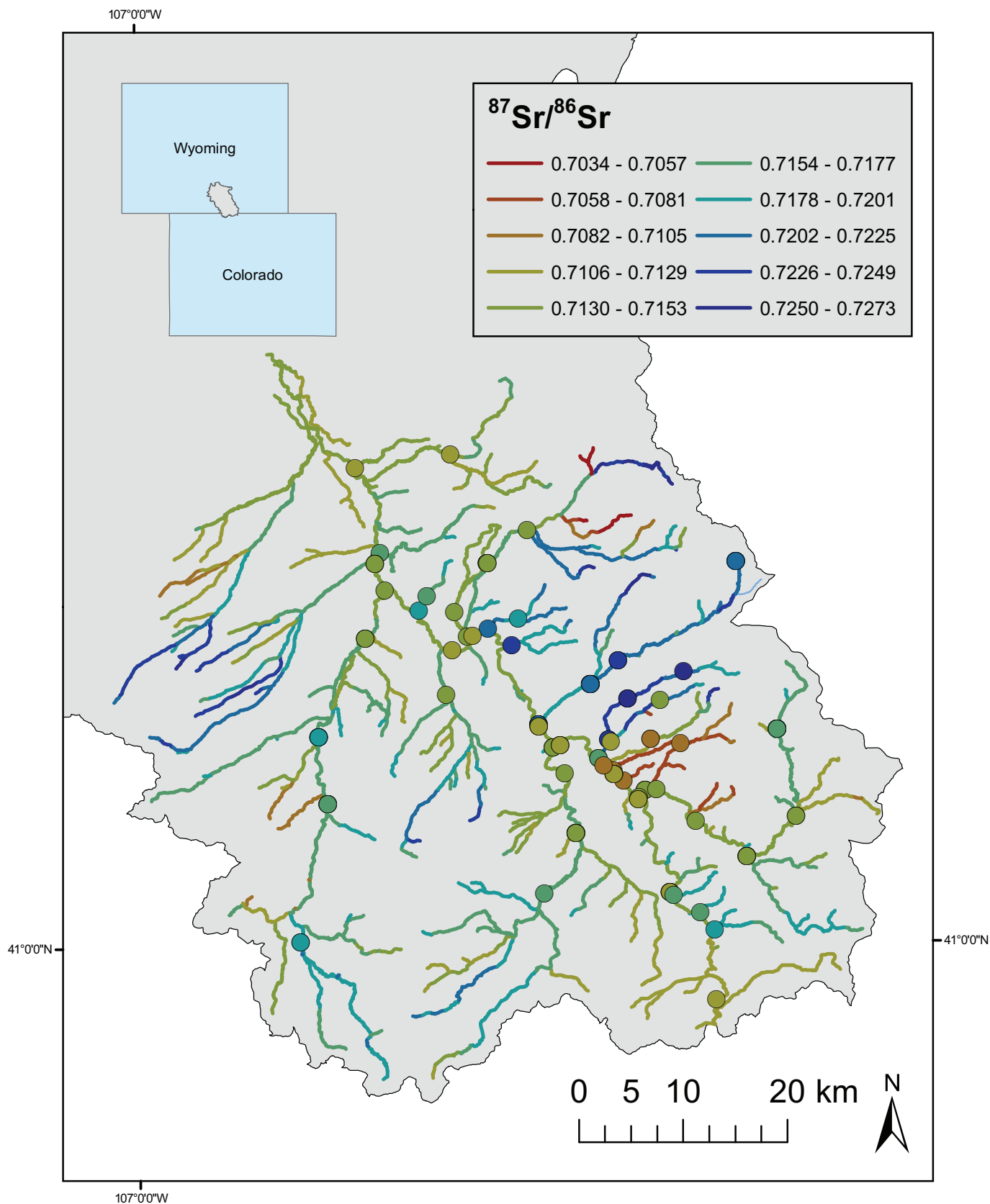
^{87}Sr/^{86}Sr models

We built and compared ^{87}Sr/^{86}Sr BRR and SSN models and used the BRR model to build a ^{87}Sr/^{86}Sr isoscape of the UNPR Basin for watersheds greater than 6 km^2. More details on BRR and SSN models will follow in later sections. Prior to modeling, we split the data into development and validation data sets. To establish our validation data set, we randomly selected eight tributaries and then randomly selected one sampling location on each of the eight tributaries. The other 51 observations served as the development data set.

The SSN model required a GIS referenced landscape network that incorporated information on stream source, flow direction, confluences, and stream outlets. Both modeling approaches required establishing and summarizing watershed bedrock lithology and landscape covariates at observation and estimation locations across the UNPR Basin. To establish stream network observation and estimation locations, build the landscape network, and summarize watershed covariates, we obtained a publicly available stream network of the UNPR Basin from the NorWeST stream temperature prediction effort (http://www.fs.fed.us/rm/boise/AWAE/projects/NorWeST.html; Isaak et al. 2016). For both modeling approaches, we used the midpoint of each 1 km stream segment in the NorWeST stream network as estimation locations. We selected the midpoint of the NorWeST stream segment that our observation points were located on to serve as our observation locations; this resulted in a maximum shift in observed sampling location of 0.5 km, but allowed us to incorporate covariates (i.e., slope and precipitation) embedded in the NorWest stream network.

To build the landscape network and delineate the upstream watershed area for observation and estimation locations, we obtained US Geological Survey digital elevation models (https://viewer.nationalmap.gov) and integrated these with the NorWesST stream network using the Spatial Tools for the Analysis of River Systems (STARS) toolbox in ArcGIS 10.2 (Peterson and Ver Hoef 2014).

Lithology and landscape covariates

We used the STARS toolbox to calculate the percent area of each rock type located upstream of every estimation and observation point along the stream network. Predominant lithology designation was obtained from the Preliminary Integrated Geologic Map Databases for the United States (https://mrdata.usgs.gov/geology/state/; Stoeser et al. 2005). In addition to lithology, we selected four landscape covariates (local relief, percent glaciated, average slope, and accumulated precipitation) to include in our models (for variable descriptions see Text S1[1]; Mears 2001; Mckay et al. 2012; Brennan et al. 2016).

Bayesian ridge regression (BRR)

We used the development data set and the BRR algorithm with tenfold cross-validation in the R version 3.3.0 (R Core Team 2016) caret package (Kuhn 2017) to develop two sets of models (initial and candidate). BRR algorithms use supervised learning (Olden et al. 2008), through k-fold cross-validation, to model the relationship between inputs and known outputs (Kuhn 2008). Because the BRR algorithm, like many machine learning algorithms, relies on supervised learning to tune model parameters, final model parameters will vary slightly with each run of the BRR algorithm. To quantify how this variance impacts model output, we ran the BRR algorithm 1000 times using covariates from the best-performing model. We then ran the development and validation data sets through the 1000 model iterations and calculated the SD of the r^2 between modeled and observed ^{87}Sr/^{86}Sr and the SD of the residual SE. Also important to note is that the BRR algorithm in the caret package requires centered and scaled predictors; therefore, we scaled and centered all input variables prior to modeling (Kuhn 2008).

Our initial model set ($n = 4$) incorporated predominant lithology found at greater than 5%, 10%, 20%, or 25% in the watershed as covariates. The candidate model set ($n = 9$) included all lithology covariates from the best-performing initial model and different combinations of landscape covariates (i.e., local relief, percent glaciated, average slope, and accumulated precipitation).

To select the best-performing model, we applied all the models to the validation data set and estimated ^{87}Sr/^{86}Sr at the eight validation locations. We then regressed observed ^{87}Sr/^{86}Sr against estimated ^{87}Sr/^{86}Sr and assumed the best-performing model was the one that maximized the goodness of fit between observed and estimated ^{87}Sr/^{86}Sr (for a complete list of candidate models, see Tables S1–S2[1]; for example code see Text S2[1]).

We used the best-performing model in the candidate model set to estimate ^{87}Sr/^{86}Sr at estimation locations in the stream network. We assumed model error was equal to the SE of the absolute difference between observed and estimated ^{87}Sr/^{86}Sr of the validation data set.

Spatial stream network (SSN) model

To compare the relative performance of the BRR model with that of a SSN model, we developed a ^{87}Sr/^{86}Sr SSN model. We used the development data set and the SSN package (Ver Hoef et al. 2014) in R version 3.3.0 (R Core Team 2016) to develop two sets of models (initial and candidate). SSN model development largely followed the methods outlined in Brennan et al. (2016). SSN models use a generalized linear mixed model framework that incorporates linear spatial relationships to model the relationship between inputs and known outputs (Peterson et al. 2013).
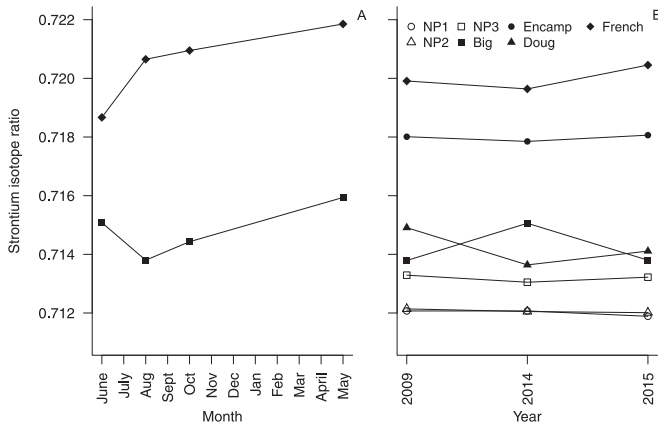
Similar to above, our initial model set ($n = 4$) incorporated predominant lithology found at greater than 5%, 10%, 20%, or 25% in the watershed as covariates. We ran the initial SSN model set with an exponential tail-up (flow-connected) autocovariance function. The candidate model set ($n = 7$) included all lithology covariates from the best-performing initial model and different combinations of landscape covariates and autocovariance functions. We did not include accumulated precipitation because this information was embedded in the SSN spatial weighting scheme. We used AIC (Akaike information criterion) to compare models and select the top model in each model set (Tables S3–S4[1]).

Similar to Brennan et al. (2016), we based spatial weights of the SSN on the product of modeled [Sr] (see Brennan et al. 2016 for methods to model [Sr]) and accumulated precipitation. Unlike in Brennan et al. (2016), we only considered exponential tail-up (flow-connected) and Euclidian autocovariance functions for all candidate models because we did not observe spatial correlation for flow-unconnected pairs (Fig. S2[1]; Peterson et al. 2013).

Inferred fish origin

Using ^{87}Sr/^{86}Sr samples and the BRR ^{87}Sr/^{86}Sr isoscape, we developed three scenarios of described spatial heterogeneity to examine the implications of inferring fish origin at increasing scales of described spatial ^{87}Sr/^{86}Sr heterogeneity. In scenario A, we used one ^{87}Sr/^{86}Sr sample from each of the 17 UNPR tributaries (collected near the confluence). In scenario B, we increased the described spatial heterogeneity by incorporating all 48 ^{87}Sr/^{86}Sr samples collected at one to five locations in the 17 tributaries. In scenario C, we again increased the described spatial heterogeneity and used estimated ^{87}Sr/^{86}Sr values from the BRR strontium isoscape in the 17 tributaries. For all scenarios, we defined each site by a uniform distribution. In scenarios A and B, the width of the uniform distribution was equal to the maximum observed year to year variability (±SD 0.00073). In scenario C, the width of the uniform distribution was equal to the BRR model error. BRR model error was equal to the SE of the absolute difference between observed and estimated ^{87}Sr/^{86}Sr of the validation data set (±0.00106). We did not explicitly incorporate temporal variation in scenario C because model error was larger than the observed temporal variation, thus overwhelming temporal variation.

932

Can. J. Fish. Aquat. Sci. Vol. 76, 2019

Fig. 2. Surface water ^{87}Sr/^{86}Sr seasonal variation (A) was higher than surface water ^{87}Sr/^{86}Sr year to year variation (B). Refer to Materials and methods for description of sampling sites.

Fig. 3. Model performances of the Bayesian ridge regression model (BRR) (A) and the spatial stream network model (SSN) (B) were comparable. Observed versus estimated ^{87}Sr/^{86}Sr values were plotted for both development and validation data sets. The solid lines are the 1:1 lines between observed strontium isotope ratios and estimated strontium isotope ratios.

We then created a hypothetical otolith ^{87}Sr/^{86}Sr data set (100 equally spaced ^{87}Sr/^{86}Sr values across the strontium gradient) and assessed the number of tributaries that each sequenced ^{87}Sr/^{86}Sr value overlapped for the three scenarios of described spatial heterogeneity. We considered a site, and thus a tributary, as a potential fish origin if the hypothetical otolith value fell within the bounds of a site's uniform distribution.

Results

^{87}Sr/^{86}Sr temporal variation

We observed both seasonal and year to year variation in ^{87}Sr/^{86}Sr, with greater seasonal variation than year to year variation (Fig. 2). In French and Big creeks, the maximum observed difference in ^{87}Sr/^{86}Sr between seasons (0.00318 and 0.00214, respectively) was higher than between years (0.00081 and 0.00127, respectively). Year to year variation in ^{87}Sr/^{86}Sr signatures was largest for Big Creek (0.71422 ± 0.00073) and smallest for the North Platte River (0.71207 ± 0.00006). The mean SD in strontium isotope ratios between seasons was 0.00134, while between years it was 0.00031. When samples from the North Platte River were excluded, the mean SD between years increased to 0.00047.
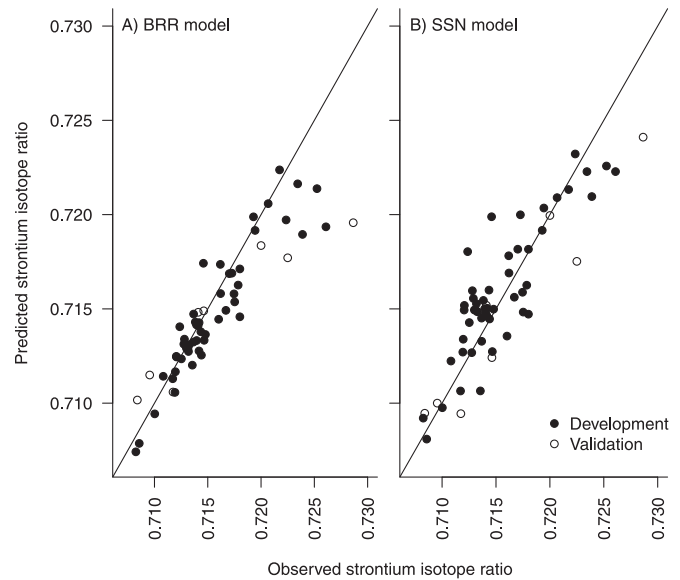
^{87}Sr/^{86}Sr models

BRR

The top BRR model for estimating ^{87}Sr/^{86}Sr throughout the UNPR Basin included all rock types found at greater than 10% in any watershed and accumulated precipitation (Fig. 1; Table S2[1]). In this model the covariates explained 86.85% (SD 0.03) of the variation in ^{87}Sr/^{86}Sr of the development data set. The r^2 between modeled and observed ^{87}Sr/^{86}Sr of the development and validation data sets was 0.93 (SD 0.0006) and 0.90 (SD 0.0056), and the residual standard error was 0.00098 (SD 0.00004) and 0.00173 (SD 0.00004), respectively (Fig. 3). Model error was equal to ±0.00106.

SSN model

The top SSN model for estimating ^{87}Sr/^{86}Sr throughout the UNPR Basin included all rock types found at greater than 10% in any watershed and average slope (Table S4[1]). In this model the fixed effects explained 79% of the variation in ^{87}Sr/^{86}Sr, and the tail-up autocovariance explained 20% of the variance. Using the best model, the r^2 between the modeled and observed ^{87}Sr/^{86}Sr of the development and validation data sets was 0.74 and 0.89 and the residual SE was 0.00203 and 0.00228, respectively (Fig. 3). Model error was equal to ±0.00086.

Inferred fish origin

Increasing described strontium spatial heterogeneity revealed large longitudinal variation within tributaries and large overlap in ^{87}Sr/^{86}Sr between tributaries (Fig. 4). Accounting for temporal and longitudinal variation along tributaries increased the number of tributaries a hypothetical fish overlapped in ^{87}Sr/^{86}Sr signatures (Fig. 4). In scenario A, we accounted for temporal variation but did not account for longitudinal variation, and fish shared a ^{87}Sr/^{86}Sr signature with zero to four tributaries. In scenario B, we accounted for both temporal and longitudinal variation, and fish shared a ^{87}Sr/^{86}Sr signature with zero to seven tributaries. In scenario C, we used continuous estimated ^{87}Sr/^{86}Sr to quantify longitudinal variation, and fish shared a ^{87}Sr/^{86}Sr signature with zero to ten tributaries. In scenario C, we did not explicitly account for temporal variation because model error was greater than observed temporal variation and absorbed the influence of temporal variation on the accuracy of inferred fish movement.

Discussion

^{87}Sr/^{86}Sr temporal variation

We observed higher site-specific ^{87}Sr/^{86}Sr seasonal variation than site-specific ^{87}Sr/^{86}Sr year to year variation, as was also seen by Kennedy et al. (2000) and Crook et al. (2017). But the degree of temporal stability varied by orders of magnitude from stable to unstable across watersheds. Kennedy et al. (2000) reported that the largest seasonal difference in ^{87}Sr/^{86}Sr observed at any one site in the Connecticut River Basin, Vermont, was 0.00035. The largest seasonal difference we observed was 0.00318, in French Creek. The largest seasonal difference Crook et al. (2017) reported was 0.05155 on the Edith River in the wet–dry tropics of northern Australia. Crook et al. (2017) suggested changes in the source water (ground versus runoff) between the two extreme wet–dry seasons likely drove observed extreme seasonal variability. We hypothesize a similar mechanism is driving our observed seasonal variability. The UNPR Basin is snowmelt-driven with snowmelt runoff contributing to most flow in the spring and ground water dominating flow during the fall and winter (Miller et al. 2014). Future studies should work to understand the relationship between temporal

Fig. 4. Increasing the described spatial variation of surface water $^{87}Sr/^{86}Sr$ (I and II, scenarios A–C) increased the number of tributaries a hypothetical fish shared an environmental signature with (III). Inferring fish movement using a single sample on each tributary (scenario A) resulted in high specificity (few tributaries overlapped with the hypothetical fish's environmental signature), but likely low accuracy (the true stream of origin was not identified). Inferring fish movement using on the ground sampling, which incorporated longitudinal variation (scenario B), resulted in intermediate specificity and likely higher accuracy. Using modeled, continuous $^{87}Sr/^{86}Sr$ to describe longitudinal variation (scenario C) resulted in low specificity and likely similar accuracy to that of scenario B. Panel I shows the water $^{87}Sr/^{86}Sr$ samples used to develop each scenario, panel II shows the spatial distribution of the water samples, and panel III shows the number of tributaries hypothetical otoliths, along the strontium gradient, overlapped with, for each scenario. [Colour online.]
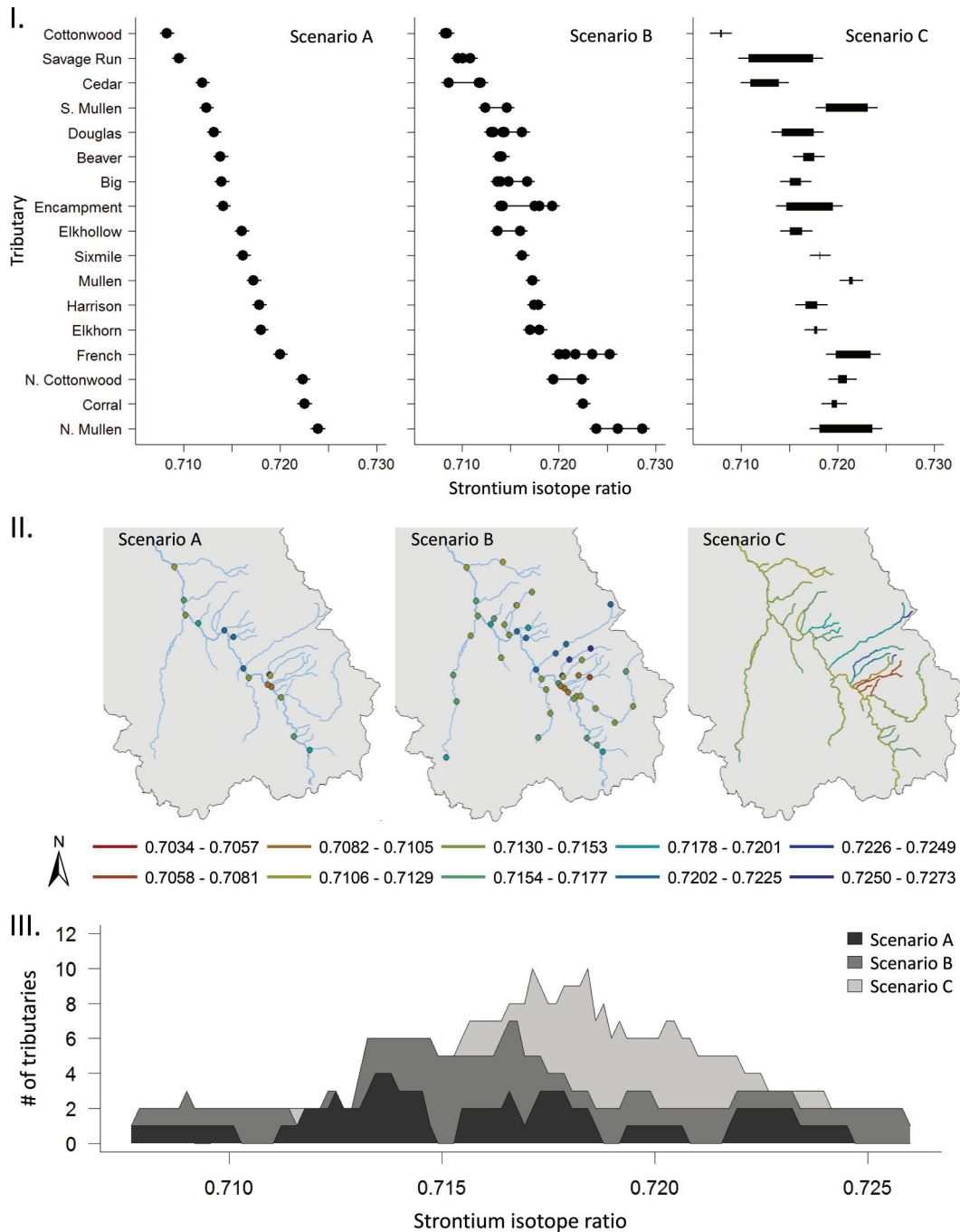
stability and variation in water inputs across climatic and geologic settings to identify regions where repeated sampling, to quantify temporal stability, is mandated and where assumptions of temporal stability hold true.

$^{87}Sr/^{86}Sr$ models

Developing $^{87}Sr/^{86}Sr$ models to create stream $^{87}Sr/^{86}Sr$ isoscapes is a new and developing research area. Our BRR modeling approach and the SSN modeling approach, presented in Brennan et al. (2016) and applied in Brennan and Schindler (2017), to building $^{87}Sr/^{86}Sr$ isoscapes are, to date, the most accurate models to estimate $^{87}Sr/^{86}Sr$ patterns in streams. But, until now, large uncertainty remained in the generalizability and accuracy of these approaches across geologic formations and geographic locations because they had not been applied outside of the Nushagak Basin.

Our results indicate publicly available stream network and lithology data can be used by researchers to build generalizable SSN and BRR models that perform well when estimating $^{87}Sr/^{86}Sr$. Both models had high model performance (r^2 of BRR and SSN validation data set modeled versus observed ratios = 0.90 and 0.89, respectively). Brennan et al. (2016) obtained similar SSN model performance when estimating $^{87}Sr/^{86}Sr$ in the Nushagak Basin, Alaska (r^2 of modeled versus observed ratios = 0.90). Both the BRR and SSN models estimated strontium isotope ratios with similar overall model error (BRR = ±0.00106; SSN = ±0.00086); however, model error was not consistent across the strontium gradient, and the region of highest model error was not consistent between the two models. The BRR model error was highest at high $^{87}Sr/^{86}Sr$ values, and the SSN model error was highest at intermediate $^{87}Sr/^{86}Sr$ values.

Differences in the magnitude of the model error across the strontium gradient and between the two modeling approaches was likely due to an interaction between the different statistical approaches and the geologic maps used. SSN models use a generalized linear mixed model framework that incorporates linear spatial relationships (Peterson et al. 2013), and BRR models use supervised learning (Olden et al. 2008) to model the relationship between inputs and known outputs. Because SSN models rely on linear spatial relationships, they have the distinct advantage of estimating spatially explicit $^{87}Sr/^{86}Sr$ estimation error (i.e., estimation locations closer to sampling locations will have smaller estimation error, while estimation locations farther from sampling locations will have larger estimation error), an important aspect when partitioning out sources of variance to probabilistically infer fish movement (see Brennan and Schindler 2017). Therefore, when modelers seek to partition out sources of variance, we recommend developing an SSN model. When partitioning out sources of variance is not necessary, we recommend developing a BRR model with the caret package (Kuhn 2017; for example code see Text S2[1]), because it is computationally simpler as it does not require a GIS-referenced landscape network and the modeling of [Sr] prior to modeling $^{87}Sr/^{86}Sr$. Because developing a BRR model is simpler, it may also serve as a powerful preliminary analysis tool to detect whether there is sufficient $^{87}Sr/^{86}Sr$ variation to justify a large-scale study.

Both modeling approaches relied on geologic maps that were created to provide standardized geologic data based on state-scale geologic lithology (Stoeser et al. 2005). These maps were not created to inform $^{87}Sr/^{86}Sr$ signatures; as such, some lithology designations may have been too broad to inform underlying $^{87}Sr/^{86}Sr$ variation. Hegg et al. (2013) found, when clustering rocks into five main rock type groups, that broad rock type classifications obscured underlying $^{87}Sr/^{86}Sr$ variation in some watersheds. While BRR and SSN models do not require clustering rock types, an improvement over Barnett-Johnson et al. (2008) and Hegg et al. (2013), it is likely some rock groupings, like metasedimentary rocks, were still too broad to inform variation in $^{87}Sr/^{86}Sr$ signatures, ultimately leading to the observed variable estimation errors.

The size of model error is currently the primary analytical limitation when using modeled $^{87}Sr/^{86}Sr$ to describe $^{87}Sr/^{86}Sr$ spatial heterogeneity across a stream network. In watersheds that contain small differences between tributary signatures, the model error associated with each estimation point may disguise true differences. Increasing the sample size and spatial representation of input data and using finer detailed bedrock geology maps would likely decrease model error within and between models. But, it is important to note, the degree to which decreasing model estimation error will improve described $^{87}Sr/^{86}Sr$ spatial heterogeneity, and our ability to infer origin is not limitless. Irrespective of model error, described $^{87}Sr/^{86}Sr$ spatial heterogeneity will remain bounded by analytical precision and natural temporal variability. Additionally, the spatial resolution of inferred fish movement is fundamentally restricted by the natural spatial discreteness of environmental signatures (see Elsdon et al. 2008).

Inferred fish origin

Increasing described spatial heterogeneity of $^{87}Sr/^{86}Sr$ signatures in the UNPR Basin likely increased the accuracy (the true stream of origin shared an overlapping signature with the fish) but decreased the specificity (many tributaries overlapped with the hypothetical fish's environmental signature) of a hypothetical fish's inferred movement. Using a single sample on each tributary to describe $^{87}Sr/^{86}Sr$ spatial heterogeneity resulted in a maximum of four tributaries overlapping with a hypothetical fish's $^{87}Sr/^{86}Sr$ signature. Without knowledge of longitudinal variation, it would be tempting to assign the hypothetical fish to one of these four tributaries. But in a connected stream network, where fish can move freely throughout the network, it would be inaccurate to assume a fish stayed at the confluence of the tributary and thus inappropriate to exclude longitudinal variation. Incorporating observed and modeled longitudinal variation increased the maximum number of tributaries with overlapping $^{87}Sr/^{86}Sr$ signatures to seven and ten tributaries, respectively. Our results indicate neglecting to incorporate longitudinal variation may lead to specific but inaccurate inferred fish origin.

Alarmingly, many otolith microchemistry studies have neglected to investigate spatial heterogeneity on multiple scales, thus failing to incorporate longitudinal variation (Elsdon et al. 2008). Elsdon et al. (2008) suggests using a nested sampling design to ensure variation in environmental signatures is described at the scale being investigated, and there is a rapidly growing body of literature to support using a continuous approach to isotope-based inferred origin–movement (i.e., BRR and SSN) to improve the accuracy of inferred movement (Wunder 2010; Brennan and Schindler 2017), and our results highlight the importance of doing so.

Conclusions

The specificity, and likely the accuracy, of inferred fish origin jointly depended on the quantification of $^{87}Sr/^{86}Sr$ spatial heterogeneity (at a scale that is relevant to fish movement) and the spatial and temporal discreteness of $^{87}Sr/^{86}Sr$. The BRR model presented in this paper is a promising, novel approach to describing the full continuous spatial heterogeneity of $^{87}Sr/^{86}Sr$ signatures and compares well with the SSN modeling technique presented in Brennan et al. (2016). Both BRR and SSN modeling techniques are not region-specific and can be applied to any watershed.

Assigning fish to $^{87}Sr/^{86}Sr$ isoscapes, developed through BRR and SSN modeling approaches, represents a powerful improvement over classic assignment methods, such as those presented in Wells et al. (2003), which rely on cluster analysis for origin assignment. Describing the continuous spatial heterogeneity of $^{87}Sr/^{86}Sr$ not only alleviates potentially unnatural groupings created by clustering data, it provides a detailed map of potential environmental signatures that can transfer to a detailed map of fish movement. However, it is important to note that in watersheds like the UNPR Basin, where spatial discreteness in $^{87}Sr/^{86}Sr$ signatures between tributaries is low, specificity of inferred fish origin will be low due to the error associated with estimated $^{87}Sr/^{86}Sr$ values. Future studies should consider both the spatial and temporal discreteness of their watershed and work to describe the full spatial heterogeneity and temporal stability of $^{87}Sr/^{86}Sr$ prior to inferring fish origin.

Author's contributions

Both authors contributed to the conception and design of the study; L.C. collected and analyzed the data; both authors contributed critically to the drafts and gave approval for publication.

Acknowledgements

References

Achord, S., Zabel, R.W., and Sandford, B.P. 2007. Migration timing, growth, and estimated parr-to-smolt survival rates of wild Snake River spring–summer Chinook salmon from the Salmon River Basin, Idaho, to the Lower Snake River. Trans. Am. Fish. Soc. **136**(1): 142–154. doi:10.1577/T05-308.1.

Barnett-Johnson, R., Pearson, T.E., Ramos, F.C., Grimes, C.B., and MacFarlane, R.B. 2008. Tracking natal origins of salmon using isotopes, otoliths, and landscape geology. Limnol. Oceanogr. **53**: 1633–1642. doi:10.4319/lo.2008.53.4.1633.

Bataille, C.P., and Bowen, G.J. 2012. Mapping $^{87}Sr/^{86}Sr$ variations in bedrock and water for large scale provenance studies. Chem. Geol. **304–305**: 39–52. doi:10.1016/j.chemgeo.2012.01.028.

Bataille, C.P., Brennan, S.R., Hartmann, J., Moosdorf, N., Wooller, M.J., and Bowen, G.J. 2014. A geostatistical framework for predicting variability in strontium concentrations and isotope ratios in Alaskan rivers. Chem. Geol. **389**: 1–15. doi:10.1016/j.chemgeo.2014.08.030.

Binder, T.R., Cooke, S.J., and Hinch, S.G. 2011. Physiological specializations of different fish groups: fish migrations. *In* Encyclopedia of fish physiology: from genome to environment. Vol. 3. *Edited by* A.P. Farrell. Elsevier Inc. pp. 1921–1927. Available from https://doi.org/10.1016/B978-0-12-374553-8.00085-X [accessed 29 January 2019].

Brennan, S.R., and Schindler, D.E. 2017. Linking otolith microchemistry and dendritic isoscapes to map heterogeneous production of fish across river basins. Ecol. Appl. **27**: 363–377. doi:10.1002/eap.1474. PMID:27875020.

Brennan, S.R., Fernandez, D.P., Zimmerman, C.E., Cerling, T.E., Brown, R.J., and Wooller, M.J. 2015. Strontium isotopes in otoliths of a non-migratory fish (slimy sculpin): Implications for provenance studies. Geochim. Cosmochim. Acta, **149**: 32–45. doi:10.1016/j.gca.2014.10.032.

Brennan, S.R., Torgersen, C.E., Hollenbeck, J.P., Fernandez, D.P., Jensen, C.K., and Schindler, D.E. 2016. Dendritic network models improve isoscapes and quantify influence of landscape and in-stream processes on strontium isotopes in rivers. Geophys. Res. Lett. **43**(10): 5043–5051. doi:10.1002/2016GL068904.

Brown, J.A. 2006. Using the chemical composition of otoliths to evaluate the nursery role of estuaries for English sole *Pleuronectes vetulus* populations. Mar. Ecol. Prog. Ser. **306**: 269–281. doi:10.3354/meps306269.

Cooke, S.J., Paukert, C., and Hogan, Z. 2012. Endangered river fish: factors hindering conservation and restoration. Endang. Species Res. **17**: 179–191. doi:10.3354/esr00426.

Crook, D.A., Lacksen, K., King, A.J., Buckle, D.J., Tickell, S.J., Woodhead, J.D., Maas, R., Townsend, S.A., and Douglas, M.M. 2017. Temporal and spatial variation in strontium in a tropical river: implications for otolith chemistry analyses of fish migration. Can. J. Fish. Aquat. Sci. **74**(4): 533–545. doi:10.1139/cjfas-2016-0153.

Dorval, E., Jones, C.M., Hannigan, R., and van Montfrans, J. 2005. Can otolith chemistry be used for identifying essential seagrass habitats for juvenile spotted seatrout, *Cynoscion nebulosus*, in Chesapeake Bay? Mar. Freshw. Res. **56**(5): 645–653. doi:10.1071/MF04179.

Elsdon, T.S., Wells, B.K., Campana, S.E., Gillanders, B.M., Jones, C.M., et al. 2008. Otolith chemistry to describe movements and life-history parameters of fishes: hypotheses, assumptions, limitations and inferences. Oceanogr. Mar. Biol. **46**: 297–330. doi:10.1201/9781420065756.ch7.

Gibson-Reinemer, D.K., Johnson, B.M., Martinez, P.J., Winkelman, D.L., Koenig, A.E., and Woodhead, J.D. 2009. Elemental signatures in otoliths of hatchery Rainbow Trout (*Oncorhynchus mykiss*): distinctiveness and utility for detecting origins and movement. Can. J. Fish. Aquat. Sci. **66**(4): 513–524. doi:10.1139/F09-015.

Gross, M.R., Coleman, R.M., and McDowall, R.M. 1988. Aquatic productivity and the evolution of diadromous fish migration. Science, **239**(4845): 1291–1293. doi:10.1126/science.239.4845.1291. PMID:17833216.

Hegg, J.C., Kennedy, B.P., and Fremier, A.K. 2013. Predicting strontium isotope variation and fish location with bedrock geology: understanding the effects of geologic heterogeneity. Chem. Geol. **360–361**: 89–98. doi:10.1016/j.chemgeo.2013.10.010.

Hodge, B.W., Wilzbach, M.A., Duffy, W.G., Quinones, R.M., and Hobbs, J.A. 2016. Life history diversity in Klamath River Steelhead. Trans. Am. Fish. Soc. **145**(2): 227–238. doi:10.1080/00028487.2015.1111257.

Hutchison, M., Butcher, A., Kirkwood, J., Mayer, D., Chilcott, K., and Backhouse, S. 2008. Mesoscale movement of small and medium-sized fish in Murray-Darling Basin. Available from the Murray–Darling Basin Commission office, Canberra, ACT. Publ. 41/08.

Isaak, D., Nagel, D., Groce, M., Wenger, S., Peterson, E., et al. 2016. A thermal map for all *Wyoming* streams [online]. Available from https://www.fs.fed.us/rm/boise/AWAE/projects/stream_temp/publications.html [accessed 11 August 2018].

Kanno, Y., Letcher, B.H., Coombs, J.A., Nislow, K.H., and Whiteley, A.R. 2014. Linking movement and reproductive history of Brook Trout to assess habitat connectivity in a heterogeneous stream network. Freshw. Biol. **59**(1): 142–154. doi:10.1111/fwb.12254.

Kennedy, B.P., Blum, J.D., Folt, C.L., and Nislow, K.H. 2000. Using natural strontium isotopic signatures as fish markers: methodology and application. Can. J. Fish. Aquat. Sci. **57**(11): 2280–2292. doi:10.1139/f00-206.

Kuhn, M. 2008. Building predictive models in R using the caret Package [online]. J. Stat. Softw. **28**(5). Available from https://www.jstatsoft.org/index [accessed 15 July 2017].

Kuhn, M. 2017. Caret: Classification and Regression Training. R package version 6.0-76 [online]. Available from http://CRAN.R-project.org/package=caret [accessed 15 July 2017].

Lucas, M.C., and Baras, E. 2000. Methods for studying spatial behaviour of freshwater fishes in the natural environment. Fish Fish. **1**: 283–316. doi:10.1046/j.1467-2979.2000.00028.x.

McKay, L., Bondelid, T., Dewald T., Johnston, J., Moore, R., and Rea, A. 2012. NHD*Plus* Version 2: User guide [online]. US Environmental Protection Agency. Available from https://s3.amazonaws.com/nhdplus/NHDPlusV21/Documentation/NHDPlusV2_User_Guide.pdf [accessed 21 January 2018].

Mears, B., Jr. 2001. Glacial records in the Medicine Bow Mountains and Sierra Madre of southern Wyoming and adjacent Colorado, with a traveler's guide to their sites. Wyoming State Geological Survey Public Information Circular 41, Laramie, Wyoming.

Miller, M.P., Susong, D.D., Shope, C.L., Heilweil, V.M., and Stolp, B.J. 2014. Continuous estimation of baseflow in snowmelt-dominated streams and rivers in the Upper Colorado River Basin: a chemical hydrograph separation approach. Water Resour. Res. **50**(8): 6986–6999. doi:10.1002/2013WR014939.

Muhlfeld, C.C., Thorrold, S.R., McMahon, T.E., and Marotz, B. 2012. Estimating westslope cutthroat trout (*Oncorhynchus clarkii lewisi*) movements in a river network using strontium isoscapes. Can. J. Fish. Aquat. Sci. **69**(5): 906–915. doi:10.1139/f2012-033.

Munro, A.R., McMahon, T.E., and Ruzycki, J.R. 2005. Natural chemical markers identify source and date of introduction of an exotic species: Lake Trout (*Salvelinus namaycush*) in Yellowstone Lake. Can. J. Fish. Aquat. Sci. **62**(1): 79–87. doi:10.1139/f04-174.

Olden, J.D., Poff, N.L., and Bestgen, K.R. 2006. Life-history strategies predict fish invasions and extirpations in the Colorado River Basin. Ecol. Monogr. **76**(1): 25–40. doi:10.1890/05-0330.

Olden, J.D., Lawler, J.J., and Poff, N.L. 2008. Machine learning methods without tears: a primer for ecologists. Q. Rev. Biol. **83**(2): 171–193. doi:10.1086/587826. PMID:18605534.

Peterson, E.E., and Ver Hoef, J.M. 2014. STARS: an ArcGIS toolset used to calculate the spatial information needed to fit spatial statistical models to stream network data [online]. J. Stat. Softw. **56**(2). Available from https://www.jstatsoft.org/index [accessed 10 February 2017].

Peterson, E.E., Ver, Hoef, J.M., Isaak, D.J., Falke, J.A., Fortin, M., et al. 2013. Modeling dendritic ecological networks in space: an integrated network perspective. Ecol. Lett. **16**(5): 707–719. doi:10.1111/ele.12084. PMID:23458322.

R Core Team. 2016. R: a language and environment for statistical computing [online]. R Foundation for Statistical Computing, Vienna, Austria. Available from https://www.R-project.org/ [accessed 15 June 2016].

Stoeser, D.B., Green, G.N., Morath, L.C., Heran, W.D., Wilson, A.B., et al. 2005. Preliminary integrated geologic map databases for the United States Central States: Montana, Wyoming, Colorado, New Mexico, Kansas, Oklahoma, Texas, Missouri, Arkansas, and Louisiana [online]. US Geological Survey Open-File Report 1351. US Geological Survey, Reston, Va. Available from https://pubs.usgs.gov/of/2005/1351/ [accessed 11 August 2018].

Taucher, P., Bartos, T.T., Taboga, K.G., Hallberg, L.L., Clark, M.L., et al. 2013. Platte River Basin water plan update groundwater study level I (2009–2013). Wyoming State Geological Survey Publication. Prepared for Wyoming Water Development Commission, Laramie, Wyoming.

Ver Hoef, J.M., Peterson, E.E., Clifford, D., and Shah, R. 2014. SSN: An R package for spatial statistical modeling on stream networks [online]. J. Stat. Softw. **56**(3). Available from https://www.jstatsoft.org/index [accessed 17 March 2017].

Wells, B.K., Rieman, B.E., Clayton, J.L., Horan, D.L., and Jones, C.M. 2003. Relationships between water, otolith and scale chemistries of Westslope Cutthroat Trout from the Coeur d'Alene River, Idaho: the potential application of hard-part chemistry to describe movements in freshwater. Trans. Am. Fish. Soc. **132**: 409–424. doi:10.1577/1548-8659(2003)132<0409:RBWOAS>2.0.CO;2.

Whitledge, G.W., Johnson, B.M., Martinez, P.J., and Martinez, A.M. 2007. Sources of nonnative centrarchids in the Upper Colorado River revealed by stable

936

Can. J. Fish. Aquat. Sci. Vol. 76, 2019

isotope and microchemical analyses of otoliths. Trans. Am. Fish. Soc. **136**(5): 1263–1275. doi:10.1577/T06-045.1.

Wunder, M.B. 2010. Using isoscapes to model probability surfaces for determining geographic origins. *In* Isoscapes: understanding movement, pattern, and process on earth through isotope mapping. *Edited by* J.B. West, G.J. Bowen, T.E. Dawson, and K.P. Tu. Springer, Berlin, Germany. pp. 251–270.

Young, M.K., Wilkison, R.A., Phelps, J.M., III, and Griffith, J.S. 1997. Contrasting movement and activity of large brown trout and rainbow trout in Silver Creek, Idaho. Gt. Basin Nat. **57**(3): 238–244.

Zlokovitz, E.R., Secor, D.H., and Piccoli, P.M. 2003. Patterns of migration in Hudson River striped bass as determined by otolith microchemistry. Fish. Res. **63**: 245–259. doi:10.1016/S0165-7836(03)00069-9.